JOURNAL OF APPLIED ELECTROCHEMISTRY **27** (1997) 185–191

Internal stress and magnetic properties of electrodeposited amorphous Fe–P alloys

S. ARMYANOV, S. VITKOVA, O. BLAJIEV

Institute of Physical Chemistry, Bulgarian Academy of Sciences, Sofia 1113, Bulgaria

Received 11 March 1996; revised 28 June 1996

Amorphous Fe–P alloys were electrodeposited under galvanostatic conditions at a current density of 10 A dm^{-2} from sulfate–chlorine solutions containing β-alanine and glycine, as well as hypophosphoric acid. It was established that an increase in the deposition temperature from 50 to 60°C causes an increase in the deposition rate and a substantial rise in current efficiency and internal stress (IS). With pH increase from 2.0 to 3.0 the phosphorus content decreases, current efficiency almost doubles and there is a substantial drop in IS. It is assumed that a higher electrolyte acidity enhances hydrogen occlusion in the coating, which then desorbs from the deposit creating tensile IS. The same correlation between IS and current efficiency is observed when glycine concentration varies. A profile of residual IS is plotted illustrating the IS distribution throughout the deposit thickness. When the samples are magnetized in the coating plane, the shape of the hysteresis loop indicates perpendicular magnetic anisotropy. This is due to the columnar structure observed in scanning electron micrographs of the coating cross-sections. There is a linear dependence between IS and coercivity of amorphous Fe–P alloys deposited under different conditions.

1. Introduction

Amorphous alloys are interesting materials from a technological standpoint. They possess high corrosion resistance and attractive magnetic parameters, such as high permeability, low hysteresis losses and other valuable technological properties. Ferromagnetic amorphous alloys based on iron group metals can be used for electronic components, transformers, memory devices etc. [1,2]. Amorphous alloys are also used to experimentally verify the theoretical predictions of a number of properties [1,3]. Rapid quenching, electrodeposition, electroless plating and sputtering are used for preparation of amorphous alloys.

The advantage of rapidly quenched glassy metals lies in the possibility of alloying 5–6 components to modify the properties to a great extent and to obtain materials of desired physical and chemical parameters. Glassy metals obtained by rapid quenching are usually in the form of narrow ribbons which reduces their area of application.

Plating (by electro and electroless deposition) of amorphous alloys is suitable for treatment of parts of complex shape and for preparation of foils with desired thickness. Moreover, knowledge of the interrelations between plating conditions, the composition and structure, and the properties may help produce coatings with desired behaviour and parameters. All these circumstances contribute to preferring plating as a method for glassy metal preparation. Occasionally the realization of these advantages is difficult because of poor adhesion to the substrate often caused by internal stress (IS). This calls for a systematic study of IS in these coatings, investigating their relation to plating parameters and alloy composition. The possible application of the alloys in electronic and electrical industries demands examination of their magnetic properties. It is also interesting to study the interrelation between magnetic properties and IS.

Rapidly quenched Fe-P alloys are magnetically soft materials with coercivity 0.01–0.1 Oe [3]. It would be interesting to compare magnetic properties of Fe–P alloys of the same composition, but obtained by different techniques: rapid quenching and electrodeposition. This task requires data on the magnetic properties of plated alloys. Investigation of the dependence of magnetic properties on the plating conditions is also desirable. Solutions for electrodeposition of amorphous alloys Fe–P are acidic and, besides a salt of iron and hypophosphite, contain a complexing agent to prevent precipitation of insoluble iron hydroxides [4–9].

It is also known that the nature of the complexors in the solution and their concentration in it exert a very strong influence on all physical, mechanical and chemical properties of the electrodeposited coatings. Glycine and β-alanine are used as complexing agents in an electrolyte for deposition of Fe–P[8]. This patent mentions that this couple of complexors ensures low values of IS, but no data are provided, and the structure and magnetic properties are not described.

The aim of this study is to investigate the variation of internal stress and magnetic properties of amorphous Fe–P alloys with varying plating conditions (besides the current density) and concentration of the two above-mentioned complexors. The interrelation between magnetic properties and IS is also studied.

0021-891X

2. Experimental technique

The investigated alloys were electrodeposited from a solution containing $FeSO_4.7H_2O$ (167 g dm^{-3}), $FeCl_2$(83 ml dm^{-3}, 30% solution of $FeCl_2$), 0 to 50 g dm^{-3} β-alanine; 0 to 50 g dm^{-3} glycine, $NaH_2PO_2 \cdot H_2O$ (13 g dm^{-3}), H_3PO_2 (33g dm^{-3} 50% solution). The acidity interval is very narrow because at pH < 1.9 the current efficiency is very low and at pH > 3 the amount of phosphorus in the alloys decreases sharply and the coatings are no longer amorphous. This is the reason for the following selection of plating conditions: pH 1.95–3.0, temperature 50–70°C, under galvanostatic conditions at a current density of 10 A dm^{-2}. The deposition rate and current efficiency were calculated on the basis of weighing the alloy amount deposited onto a plate area of 4×10^{-4} m^2. Preliminary treatment of the samples surface comprised electrochemical degreasing in alkaline solution, etching in mixture of nitric, phosphoric and acetic acids and rinsing with distilled water.

It is possible to characterize accurately the mechanically strained state of the coating using three types of interrelated internal stress (IS): instantaneous, residual and average [10]. As a result of the deposition of the ith coating layer with thickness Δt, an instantaneous stress (σ_{ii}) is initiated in it. At continuing deposition the upper layers treat the already deposited part of the coating like a substrate and the instantaneous stresses initiated in these upper layers affect the strained state of the ith layer. At the end of the coating formation IS in the ith layer is different as compared with the instantaneous stress caused by the influence of upper layers. Finally a new value of IS is established in the ith coating layer: the residual IS (σ_i) where, besides the instantaneous stress initiated due to its deposition, the effect of all upper layers on the strained state of the layer is taken into account [10].

The bent strip (cantilever beam) technique was used for the IS measurement [10]. Electrodeposition was applied to one side of copper foils 40 mm long, 5 mm wide and 95 μm thick. The other side of the foils was insulated with varnish. Owing to the IS initiated in the coating (deposited only on the one side of the substrate) bending of the whole system occurred. One end of the substrate was clamped, the other was free to deflect. Young's modulus of the substrate was determined before plating from the deviation of the substrate's free end conditioned by the application of a force [11]. The formulae for calculation of instantaneous (σ_{ii}) and residual (σ_i) IS in case of the bent strip method are discussed elsewhere [10]. Here we show the equations used for calculation of these values. For IS, the formula given by Popereka [12] is used :

$$\sigma_{ii} = \frac{\tilde{E}_0 t_0^2}{3L^2} k_i \frac{\Delta f_i}{\Delta t} \tag{1}$$

where t_0 is the thickness of the substrate; t is the thickness of the deposit; $\tilde{E}_0 = E_0/(1 - \nu_0)$ the reduced Young's modulus of the substrate, $\tilde{E} = E/(1 - \nu)$ is the reduced Young's modulus of the coating; ν_0 and ν are Poisson's ratios of the substrate and coating, respectively; L is the bent strip length; $\triangle f_i$ the alteration of the deviation of the free bent strip end after deposition of the ith layer with thickness Δt, and k_i. is determined as follows [12]:

$$k_i = \frac{1 + 4\tilde{\gamma}\theta_i + 6\tilde{\gamma}\theta_i^2 + 4\tilde{\gamma}\theta_i^3 + \tilde{\gamma^2}\theta_i^4}{1 + 2\theta_i + \tilde{\gamma}\theta_i^2} \tag{2}$$

where $\theta_i = t_i/t_0$ and $\tilde{\gamma} = \tilde{E}/\tilde{E}_0$.

For determination of residual IS (σ_i) the following equation is applied [10]:

$$\sigma_i = \frac{\tilde{E}_0 t_0^2}{3L^2} \left\{ k_i \frac{\Delta f_i}{\Delta t_i} - \sum_{j=i+1}^{k} \frac{k_j \triangle f_j}{t_0 \tilde{\gamma}^{-1} + t_{j-1}} - \frac{6\tilde{\gamma}}{t_0^2} \left[\sum_{j=i+1}^{k} \left(t_j - \frac{\Delta t}{2} \right) \Delta f_j + \sum_{j=i+1}^{k} c_j \Delta f_j \right] \right\} \tag{3}$$

where c_j is the position of the neutral axis, measured from the surface of the substrate (near to the coating) and given by Popereka [12] as follows:

$$c_j = \frac{t_o}{2} \frac{1 - \tilde{\gamma}\theta_j^2}{1 - \tilde{\gamma}\theta_j} \tag{4}$$

The variation of residual stress through the coating thickness gives the residual stress profile or residual stress diagram [10,13]. The IS averaged through the coating thickness ($\bar{\sigma}$) is calculated in two ways: using Kouyumdjiev's formula [14] (Equation 5) and calculating the average residual stress value by means of Equation 6, where the value of σ_i computed by Equation 3 is inserted:

$$\bar{\sigma} = \frac{\tilde{E}_0 t_0^2}{3L^2} \left(\frac{1 + \gamma\tilde{\theta}^3}{1 + \theta} \right) \frac{f}{t} \tag{5}$$

$$\bar{\sigma} = \frac{1}{t} \sum_{t=1}^{k} \sigma_i \Delta t \tag{6}$$

A comparison of these two values, calculated by Equations 5 and 6, makes it possible to compare two independent approaches for IS calculation thus increasing the reliability of the results. The software for calculation of σ_{ii}, σ_i and $\bar{\sigma}$ [15] was based on the above approach to interrelation between the discussed three IS types [10].

Hysteresis loops displayed on the oscilloscope screen were used to study the magnetic properties and the equipment is described elsewhere [16]. The accuracy of the magnetic parameter determination is no less than 3%. The chemical composition of the plated alloys was evaluated by energy dispersive spectroscopy (EDS) on Jeol SuperProbe 733. The scanning electron micrographs of the samples cross sections were taken on a JSM 530 machine.

Table 1. Dependence of the composition of Fe–P coatings, the deposition rate (V_{dep}), the current efficiency (η), and the averaged through the thickness internal stress ($\bar{\sigma}$) on pH and temperature of deposition in the presence of 27 g dm^{-3} glycine and 27 g dm^{-3} β-alanine

N	*pH*	*T* / °C	V_{dep} /μm min^{-1}	η / %	*Composition* /wt %		$\bar{\sigma}$ /kg mm^{-2}
					Fe	P	
1	2.3	50	0.7	33	89	11	−0.806
2	2.3	60	1.16	44	87	13	3.94
3	2.5	50	0.6	22	85	15	0.5
4	2.5	60	1.25	45	87	13	3.0
5	2.5	70	1.28	47	83	17	3.6

3. Results and discussion

Table 1 shows that at constant acidity, when temperature is increased from 50 to 60°C, the rate of deposition rises by 80–100%, and a substantial increase in IS and current efficiency takes place. A further rise of deposition temperature from 60 to 70°C changes the above mentioned parameters slightly. The temperature increase causes a rise in the phosphorus content in the deposit.

Figure 1 shows that when pH is increased, the content of phosphorus in the deposit decreases, the current efficiency almost doubles and IS is substantially reduced. This suggests that, at higher solution acidity, the amount of hydrogen occluded in the deposit increases and its desorption subsequently causes tensile IS. This assumption is supported by the current efficiency drop with pH decrease. The role of desorption of hydrogen occluded during plating on the increase in tensile IS in electrodeposited nickel coatings is discussed elsewhere [17].

As already mentioned, the type and concentration of the complexing agents are significant for the coating properties. In this work the amorphous alloy properties were studied in the presence of β-alanine and glycine, in concentrations different from those listed in [8]. Table 2 shows that concentration changes of the complexing agents within the shown limits, as well as the substitution of β-alanine with glycine, affect the alloy composition slightly.

To establish the influence of the β-alanine and glycine concentration on IS and current efficiency, the content of one complexor was varied from 0 to 27 g dm^{-3} keeping the concentration of the other complexing agent constant at 27 g dm^{-3}. Figure 2 shows a nonmonotonic dependence of the mentioned properties on β-alanine concentration. There is a minimum in IS and a maximum in current efficiency at 10 g dm^{-3} β-alanine and, obviously, this is an optimal concentration. Increase in glycine concentration causes a deleterious effect on the coating properties, increasing IS and decreasing current efficiency almost three times. Thus the above-mentioned correlation between hydrogen and IS is confirmed.

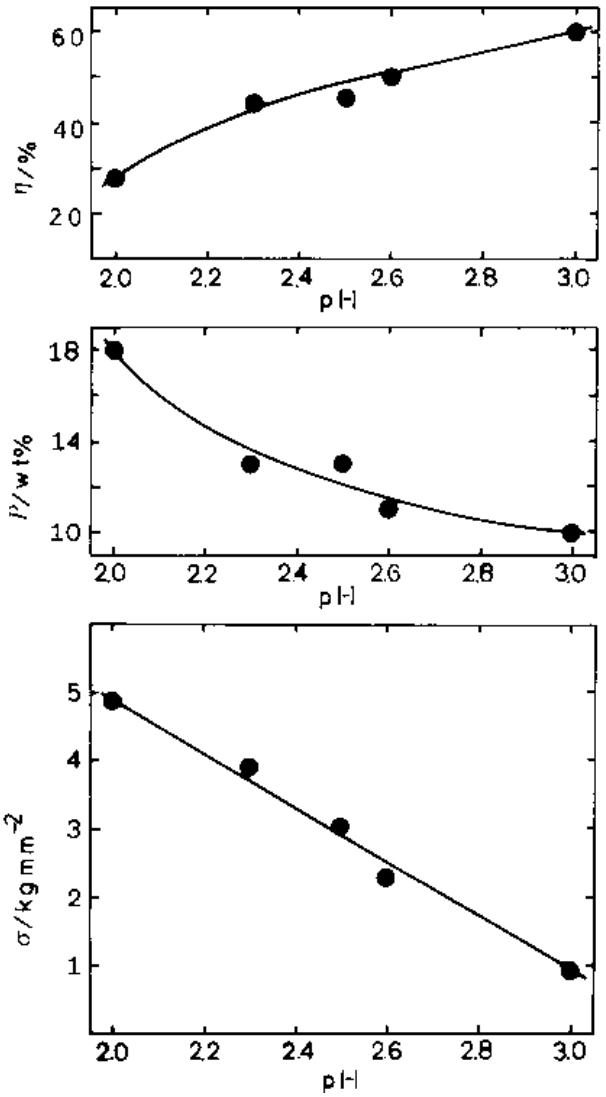

Fig. 1. Current efficiency (η), phosphorus content (wt %P), and averaged through the thickness internal stress ($\bar{\sigma}$) as a function of bath pH for electrodeposition of Fe–P coatings at temperature 60 °C in the presence of 27 g dm^{-3} glycine and 27 g dm^{-3} β-alanine.

The dependence of the deflection of the cathode free end against time during plating was used to plot the IS profile. An example of such a dependence is shown in Fig. 3. It is supposed that the coating thickness increases proportionally to the time of electrodeposition; then Equations 1 and 3 are applied.

Table 2. Influence of complexing agents concentration on current efficiency (η) and composition of Fe–P alloys at pH 2 and temperature 60 °C

Concentration of complexing agent / g dm^{-3}	η / %	*Composition* / wt %	
		Fe	*P*
30 β-alanine	22.1	85.0	15.0
40 β-alanine	26.0	84.6	15.8
50 β-alanine	28.1	87.0	13.0
30 glycine	25.0	85.0	15.0
40 glycine	25.0	85.7	14.3
50 glycine	25.6	85.0	15.0

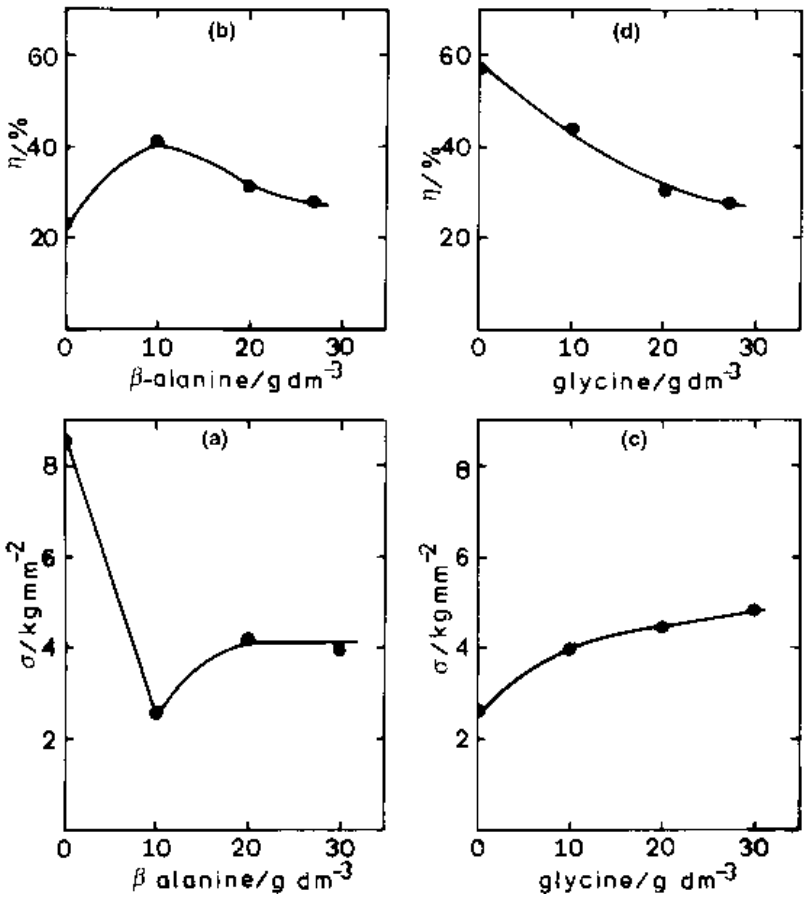

Fig. 2. Current efficiency (η) and averaged through the thickness internal stress ($\bar{\sigma}$) as a function of complexor concentration (at temperature 60 °C and pH 2): (a) and (b) at 27 g dm^{-3} glycine; (c) and (d) at 27 g dm^{-3} β-alanine.

Figure 4 illustrates three typical IS profiles for three different values of average IS. Average IS values calculated with different formulas (Equations 5 and 6) coincide within 5%.

When the average IS is not high in the layers close to the substrate, compressive residual stress is observed, despite the tensile instantaneous stress in these layers (Fig. 4(a)). The reason is that each upper layer treats the layers below itself as a substrate, causing in them IS opposite to the instantaneous [10]. In this case, in a layer close to the substrate, the stress value due to the total influence of upper layers is greater than the instantaneous IS, and the residual stress in it becomes compressive. In cases when the

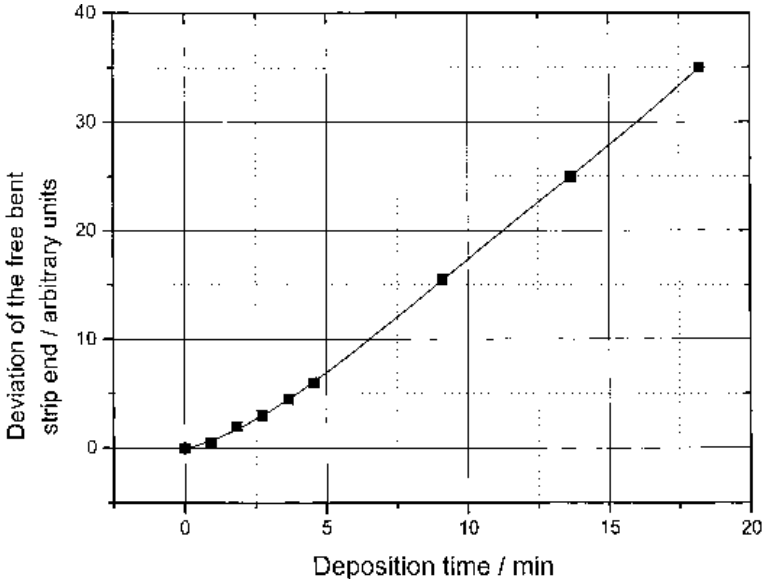

Fig. 3. Cathode free end deflection as a function of the deposition time of a coating obtained at pH 2.0, temperature 60 °C and in the presence of 10 g dm^{-3} β-alanine and 30 g dm^{-3} glycine.

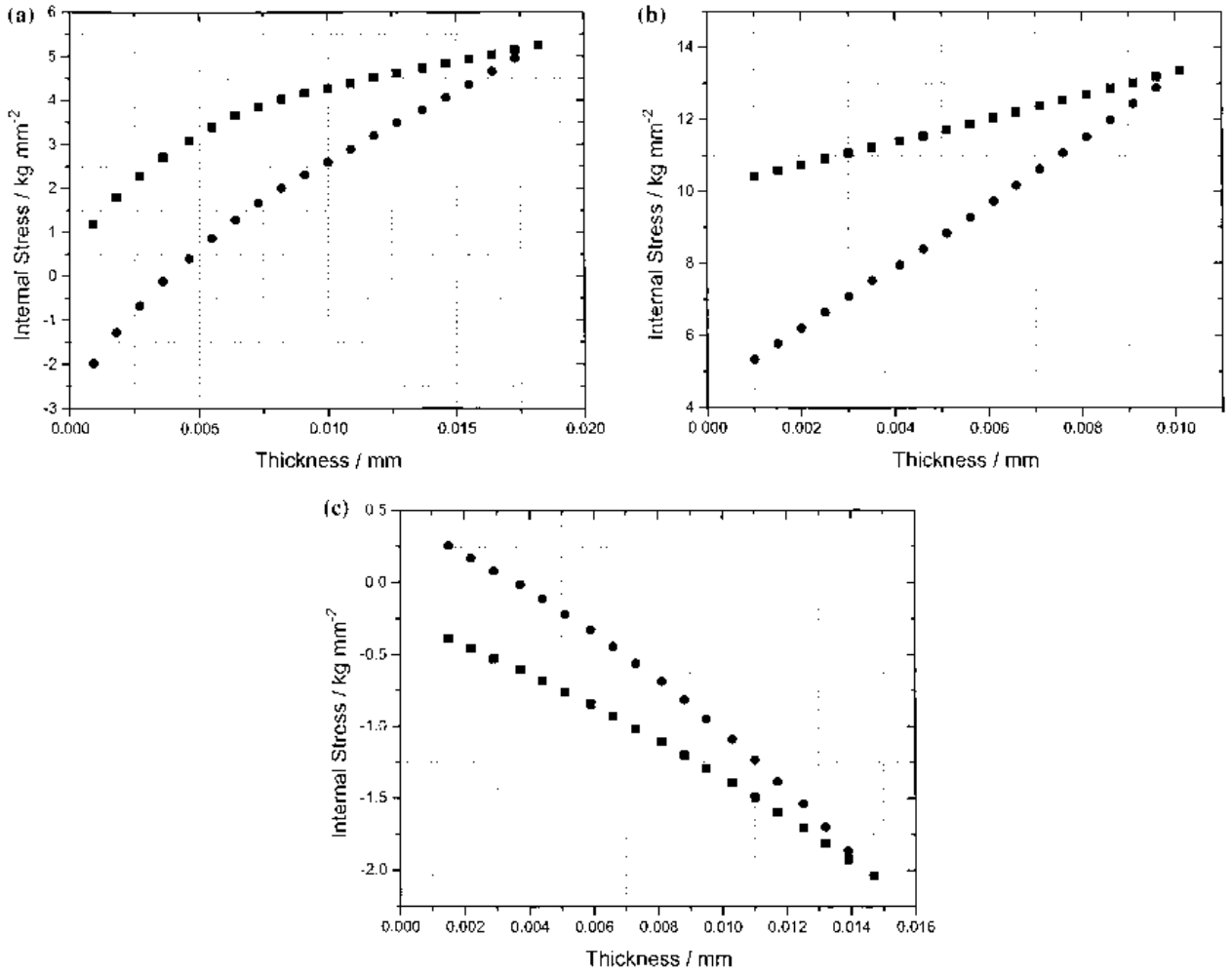

Fig 4. Profiles of instantaneous (σ_{ii}, ■) and residual (σ_i ,●) internal stress of samples obtained under the specified conditions and listed averaged through the thickness internal stress value ($\bar{\sigma}$): (a) pH 2.0, temperature 60 °C, 10 g dm^{-3} β-alanine and 30 g dm^{-3} glycine; $\bar{\sigma}$ = 2.4 kg mm^{-2}.(b) pH 2.0, temperature 60 °C, 0 g dm^{-3} β-alanine and 30 g dm^{-3} glycine; $\bar{\sigma}$ = 8.6 kg mm^{-2}. (c) pH 2.30, temperature 50 °C, 27 g dm^{-3} β-alanine and 27 g dm^{-3} glycine; $\bar{\sigma}$ = −0.81 kg mm^{-2}.

average IS is high, both instantaneous and residual stresses have the same sign (Fig. 4(b)). When the average IS is low and compressive, the instantaneous and residual stresses again possess different signs (Fig. 4(c)).

Figure 5 shows typical hysteresis loops of the layers under investigation. The magnetization of samples is in the layer plane and the hysteresis loop is strongly inclined and closed, with low squareness $\gamma = I_r/I_s$ (I_r is the remanence, I_s is the saturation magnetization). In most cases $\gamma \leq 0.5$. Such a hysteresis loop is typical for magnetization along the hard axis. There is, in general, an isotropy of properties in the electroplate plane. Thus the easy axis of magnetization should be perpendicular to the coating plane. In other words, the shape of the hysteresis loop proves the existence of perpendicular magnetic anisotropy. In this particular case the reason for its appearance is the columnar structure of the coatings, which was observed in scanning electron micrographs taken from the cross-section of plates (Fig. 6). These show columnar formations (cellular structure) and, probably the existence of oxides and hydroxides at their boundaries. Oxides and hydroxides have different magnetic properties from those of the matrix and play the role of magnetic insulators. These boundaries are oriented perpendicularly to the coating plane producing shape magnetic anisotropy [18].

As shown in Fig. 7, there is a linear dependence between the thickness-averaged IS and the coercivity of amorphous Fe–P alloys obtained under different conditions. This proves the substantial influence of another type of magnetic energy: magnetoelastic. In this case it is appropriate to express the relationship between IS and coercivity by the formula of Kersten [19]:

$$H_c \approx \lambda_s \bar{\sigma}/I_s \qquad (7)$$

where λ_s is the saturation magnetostriction.

Figure 7 also shows that at IS of zero the straight line $H_c(\bar{\sigma})$ does not cross the zero point. This means there are other factors which may cause the appearance of magnetic inhomogeneity, responsible for the magnetic hysteresis. Besides the columnar structure this could be inhomogeneity of IS, an equivalent of IS of second and third order stress in amorphous materials [20]. If their values are known, their contribution could be evaluated through a relationship

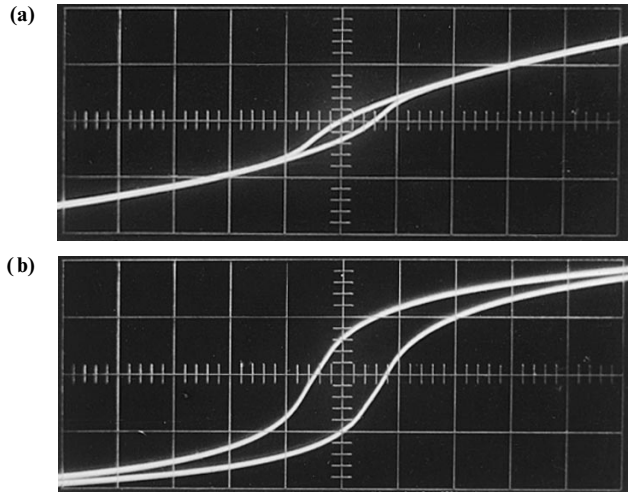

Fig. 5. Hysteresis loops (magnetic induction (arbitrary units) as a function of magnetization field (arbitrary units)) for samples obtained under the following conditions: (a) pH 2.30, temperature 50 °C, 27 g dm^{-3} β-alanine and 27 g dm^{-3} glycine; H_c=3.5 Oe. (b) pH 1.95 temperature 60 °C, 30 g dm^{-3} glycine; H_c = 8 Oe, γ=0.38.

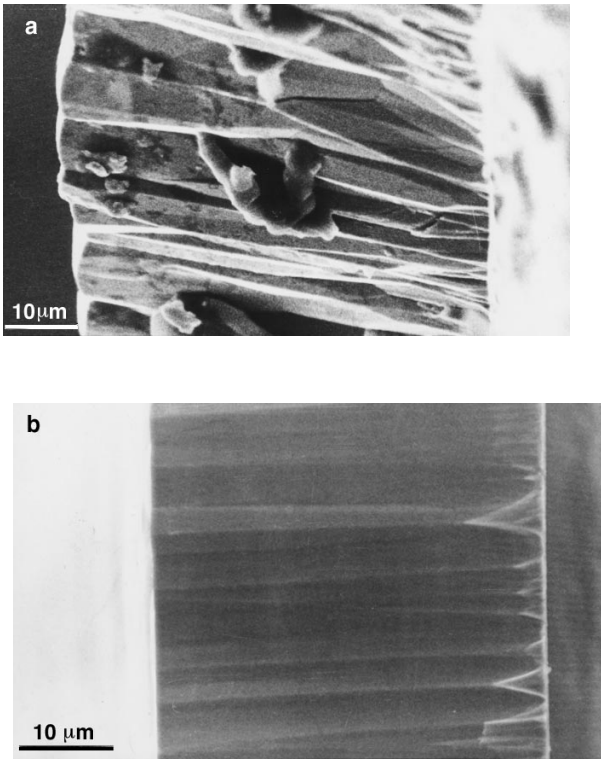

Fig. 6. Scanning electron micrographs of cross sections of samples obtained under the following conditions: (a) pH 2.0, temperature 60 °C, 0 g dm^{-3} β-alanine and 30 g dm^{-3} glycine. (b) pH 2.16, temperature 60 °C, 10 g dm^{-3} β-alanine and 30 g dm^{-3} glycine.

similar to Equation 7, where, instead of the average stress, the amplitude of IS should be inserted, which actually represents second and third order stress.

No data for magnetostriction of Fe–P were found for metallurgically obtained $Fe_{80}P_{13}C_7$; however, values of $19 \times 10^{-6}, 31 \times 10^{-6}$ and 31×10^{-6} are given [21], that is, magnetostriction of this alloy is positive and its value is significant. It is expected that magnetostriction of Fe–P will be also positive and significant. An analogous case with positive and significant magnetostriction, tensile IS and columnar structure in electrodeposition of Fe–Co alloys is considered in [22]. This shows that irrespective of the very high magnetoelastic energy (due to IS and magnetostriction), the influence of magnetostatic energy caused by shape anisotropy of the columnar structure is predominant [23]. This means that the equilibrium state of the magnetization vector is only partially determined by the magnetoelastic energy, but its influence is strong enough to affect the remagnetization processes exerting a strong influence on the coercivity. This causes the appearance of perpendicular magnetic anisotropy expressed in a strongly inclined hysteresis loop, when magnetization of samples takes place in a specified direction in the coating plane. The existence of this perpendicular magnetic anisotropy in the above mentioned electrodeposited Fe–Co is also proved by measurements made with a vibration sample magnetometer in the plane of coating and perpendicular to it [24].

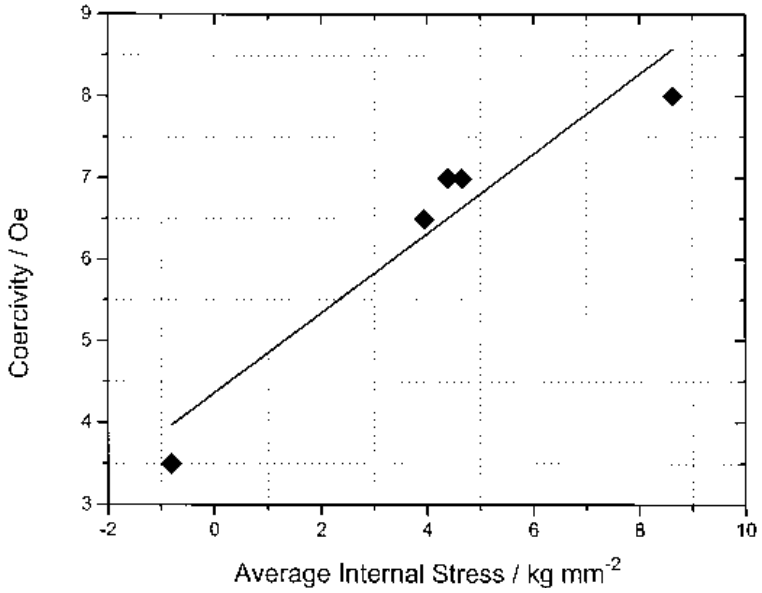

Fig. 7. Coercivity as a function of the averaged through the thickness internal stress ($\bar{\sigma}$).

4. Conclusions

(i) When pH is increased or glycine concentration is decreased there occurs a simultaneous increase in current efficiency and reduction in IS. It is suggested that at reduced current efficiency there is increased probability for hydrogen occlusion in the coating, which, after diffusing out of the deposit, causes tensile IS in it. Other mechanisms for influence of plating conditions on IS are also possible, as confirmed by the data for IS and current efficiency obtained by variation of the deposition temperature.
(ii) The shape of the hysteresis loop demonstrates the existence of perpendicular magnetic anisotropy caused by the columnar structure of the coatings. There is a linear dependence between the thickness-averaged IS and the coercivity of amorphous Fe–P alloys obtained under different conditions, which proves the influence of magnetoelastic energy on the magnetization processes.

Acknowledgements

The authors are indebted to Mrs J. Georgieva and Mrs S. Filipova for the internal stress measurements and to Mrs Ts. Tsacheva for the EDS analyses. The preparation of this paper was partially supported by the National Foundation for Scientific Research, Bulgaria under the Contract X-213.

References

[1] F. E. Luborsky (Ed.), 'Amorphous Metallic Alloys', Butterworths (1983).
[2] R. Hasegawa, *J. Magnetism Magn. Mat.* **100** (1991) 1.
[3] H. G. Guntherrodf and H. Beck (Eds), 'Glassy Metals', parts I and II, Springer, New York (1981).
[4] V. Bondar and Yu. Polukarov, *Electrokhimiya* **4** (1968) 1511.
[5] J. Logan and M. Jung, *J. Non-Cryst. Solids* **21** (1976) 151.
[6] Patent *FRG 2* 722 946 (1977); Patent *GB 1* 519 125 (1978).
[7] S. Vitkova, M. Kjuchukova, and G. Raichevski, *J. Appl. Electrochem.* **18** (1988) 683.
[8] *US Patent 4* 533 441 (1985).
[9] *US Patent 4* 746 412 (1988).
[10] S. Armyanov, *in* 'Defect Structure, Morphology and Properties of Deposits'. Proceedings of a Symposium held during Materials Week '94 in Rosemont, IL, 4–6, Oct. (1994) (edited by H. D. Merchant), A Publication of TMS, Warrendale, PA (1995) pp. 273–90.
[11] S. Timoshenko, 'Strength of Materials', D. Van Nostrand, New York (1956).
[12] Mark Ya. Popereka, *in* 'Elektroosazhdennye plenki', Kalinin; Russia, Kalinlininskij Pedagogicheskij Institut (1970) pp. 3–84 (in Russian).
[13] S. A. Armyanov, G. S. Sotirova, *Surf. Technol.* **8** (1979) 319.
[14] Ch. N. Kouyumdjiev, *ibid.* **26** (1985) 35.
[15] A. S. Armyanov, unpublished software.
[16] S. Armyanov, PhD thesis. Institute of Physics and Chemistry, Bulgarian Academy of Science, Sofia (1974).
[17] S. Armyanov, G. Sotirova-Chakarova, *J. Electrochem. Soc.* **139** (1992) 3454.
[18] Tu Chen and P. L. Cavallotti, *Appl. Phys. Lett.* **41** (1982) 205.
[19] M. Kersten, *Z. Phys.* **71** (1931) 533.
[20] S. Armyanov, G. Sotirova-Chakarova, *Metal Finish.* **90** (1992) (11) 61.
[21] F. E. Luborsky, *in* 'Feromagnetic Materials', vol. 1 (edited by E. P. Wolfarth) North-Holland, Amsterdam (1980) pp. 453–529.
[22] S. Armyanov, S. Vitkova, Z. Semenova, Yu. Polukarov, *Electrokhimiya* **13** (1977) 418.
[23] S. Armyanov, Yu. Polukarov, *Fizika Metallov Metalloved.* **46** (1978) 936.
[24] Idem, unpublished results.